

CircRIP2 aggravates the deterioration of colorectal carcinoma by negatively regulating CBFB

M. HOU¹, L.-J. ZHANG¹, J. LIU², H.-X. HU², Y.-L. ZHAO¹

¹Department of Oncology, Affiliated Hospital of North Sichuan Medical College, Nanchong, China

²Department of Oncology, Langzhong People's Hospital, Langzhong, China

Abstract. – **OBJECTIVE:** This study aims to detect expression pattern and clinical significance of circRIP2 in colorectal carcinoma (CRC). In the meantime, the regulatory effect of circRIP2 on CRC cell functions is clarified.

PATIENTS AND METHODS: Relative levels of circRIP2 in 45 cases of CRC tissues and paracancerous tissues were detected by quantitative real-time polymerase chain reaction (qRT-PCR). Its clinical significance in predicting pathological manifestations of CRC was analyzed. In vitro regulation of circRIP2 on proliferative and migratory abilities of Sw620 and HCT-116 cells was assessed by cell counting kit-8 (CCK-8), 5-Ethynyl-2'-deoxyuridine (EdU) and transwell assay, respectively. Dual-Luciferase reporter assay and rescue experiments were conducted to reveal the interaction between circRIP2 and its target gene CBFB, as well as their co-regulation on CRC cell functions. At last, in vivo regulation of circRIP2 on CRC growth in nude mice implanted with HCT-116 cells was explored.

RESULTS: CircRIP2 was upregulated in these samples of CRC tissues and cell lines. High level of circRIP2 predicted advanced staging, and high risk of distant metastasis of CRC. In vitro knockdown of circRIP2 weakened proliferative and migratory abilities in Sw620 and HCT-116 cells. CBFB was downregulated in CRC tissues, which was negatively regulated by circRIP2 as its target gene. The attenuated proliferative and migratory abilities in Sw620 and HCT-116 cells with circRIP2 knockdown were abolished by co-silence of circRIP2 and CBFB. Moreover, in vivo knockdown of circRIP2 slowed down CRC growth in nude mice, and upregulated positive expression of CBFB in xenografted CRC tissues.

CONCLUSIONS: CircRIP2 is a potential indicator for predicting tumor staging and distant metastasis of CRC. It aggravates the deterioration of CRC through negatively regulating CBFB.

Key Words:

CircRIP2, CBFB, Colorectal carcinoma.

Introduction

Globally, the incidence of colorectal carcinoma (CRC) ranks following lung carcinoma and breast cancer, which is in the second place of female cancers; and the mortality of CRC ranks fourth¹⁻³. Surgery is the first choice for early stage CRC, which is combined with post-operative comprehensive treatment, including chemotherapy, targeted therapy, etc. It effectively reduces tumor load and unblocks intestines, thus prolonging the survival of CRC patients⁴⁻⁶. Nevertheless, recurrence and metastasis largely threaten the life quality and even survival of cancer patients⁶⁻⁸. Seeking for novel biomarkers used for diagnosing CRC in the early phase and recognizing recurrent or metastatic cases is of significance to improve clinical outcomes^{9,10}.

CircRNAs are classic RNAs formed by a closed loop structure, which was first discovered in viroids in 1976^{11,12}. They are extensively distributed in both intracellular and extracellular environments, with high specificities of periods, tissues and diseases¹³. Because the deficient of 3' poly (A) and 5' cap, circRNAs are highly stable in tissues and exosomes owing to the resistance to exonucleases. As a result, circRNAs are able to be utilized as diagnostic and prognostic biomarkers for human cancers¹³⁻¹⁶. CircRIP2 is stably expressed in human bodies, which is more stable than that of linear RNA¹⁷. A previous study¹⁷ has reported its oncogenic role in bladder cancer.

CircRNAs are able to intervene gene expressions by sponging miRNAs, regulating mRNA transcription or interacting with RNAs or proteins. A small part of circRNAs can even synthesize proteins as transcription templates^{18,19}. Bioinformatic analysis predicted that CBFB shared a binding site with circRIP2 3'UTR. This study first examined expression

pattern and clinical significance of circRIP2 in CRC, and further explored its molecular mechanism.

Patients and Methods

CRC Samples

Forty-five CRC patients with surgical resection in Affiliated Hospital of North Sichuan Medical College were retrospectively analyzed. Inclusion criteria: patients with no severe diseases in other organs, and none of patients had preoperative chemotherapy/radiotherapy, endocrine or molecular targeted therapy. Exclusion criteria: patients with distant metastasis, those complicated with other malignancies, those with mental disease, those complicated with myocardial infarction, heart failure or other chronic diseases, or those previously exposed to radioactive rays. Tumor node metastasis (TNM) staging of CRC was defined by Union for International Cancer Control (UICC) criteria. CRC tissues and paracancerous tissues (normal intestinal mucosa tissues at least 5 cm from the edge of the tumor) were harvested during surgery and stored in liquid nitrogen. This investigation was approved by the research Ethics Committee of Affiliated Hospital of North Sichuan Medical College and complied with the Helsinki Declaration. Informed consent was obtained from patients.

Cell Lines and Reagents

CRC cell lines (Caco2, Sw620, HT29, HCT-8, HCT-116) and the intestinal epithelial cell line (FHC) were purchased from American Type Culture Collection (ATCC) (Manassas, VA, USA). Sw620 and Caco2 cells were cultivated in Dulbecco's Modified Eagle's Medium (DMEM) (Gibco, Rockville, MD, USA), and the others were in Roswell Park Memorial Institute-1640 (RPMI-1640) (HyClone, South Logan, UT, USA). 10% fetal bovine serum (FBS) (Gibco, Rockville, MD, USA), 100 U/mL penicillin and 100 µg/mL streptomycin were supplemented in the medium. Cell passage was conducted at 90% confluence, and those in the logarithmic growth phase were collected for experiments.

Transfection

Transfection plasmids were synthesized by GenePharma (Shanghai, China). Cells were cultured to 30-50% density in a 6-well plate, and transfected using Lipofectamine 2000 (Invitrogen, Carls-

bad, CA, USA). After 48 h cell transfection, cells were collected for verifying transfection efficacy and functional experiments.

Cell Proliferation Assay

Cells were inoculated in a 96-well plate with 2×10^3 cells/well. At day 1, 2, 3 and 4, optical density at 450 nm of each sample was recorded using the cell counting kit-8 (CCK-8) kit (Dojindo Laboratories, Kumamoto, Japan) for plotting the viability curves.

5-Ethynyl-2'-Deoxyuridine (EdU) Assay

10 µL of EdU (50 µM) was applied for cell labeling. Two hours later, cells were incubated with 4% methanol for 20 min, followed by phosphate-buffered saline (PBS) washing and incubation with Cell-Light™ EdU Apollo®488 (Life Technologies, New York, NY, USA). 4',6-diamidino-2-phenylindole (DAPI) was used for nuclei staining in the dark. Finally, cells were washed in PBS and captured for calculating EdU-positive rate.

Transwell Migration Assay

Cell suspension was prepared at 5×10^5 cells/mL. 200 µL of suspension and 700 µL of medium containing 20% FBS was respectively added on the top and bottom of a transwell insert and cultured for 48 h. Migratory cells on the bottom were induced with methanol for 15 min, 0.2% crystal violet for 20 min and captured using a microscope. Five random fields per sample were selected for capturing and counting migratory cells.

Quantitative Real-Time Polymerase Chain Reaction (qRT-PCR)

Cells were lysed using TRIzol reagent (Invitrogen, Carlsbad, CA, USA) for isolating RNAs. Qualified RNAs were reversely transcribed into complementary deoxyribose nucleic acids (cDNAs) using AMV reverse transcription kit (TaKaRa, Otsu, Shiga, Japan), followed by qRT-PCR using SYBR®Premix Ex Taq™ (TaKaRa, Otsu, Shiga, Japan). GAPDH was the internal reference. Each sample was performed in triplicate, and relative level was calculated by $2^{-\Delta\Delta Ct}$. circRIP2: Forward: 5'-CACCATCAAGTTC-GTTTGCT-3', reverse: 5'-GGCTGGTAGTGG-CAGTGATT-3'; CFBF: Forward: 5'-GAGCCG-CGAGTGTGAGATTA-3', reverse: 5'-CCAGACAGCCCATACCATCC-3'; GAPDH: Forward: 5'-TACTAGCGGTTTTACGGGCG-3', reverse: 5'-TCGAACAGGAGGAGCAGAGAGCGA-3'.

Western Blot

Cells were lysed in radioimmunoprecipitation assay (RIPA) (Beyotime, Shanghai, China) on ice for 15 min, and the mixture was centrifuged at 14000×g, 4°C for 15 min. The concentration of cellular protein was determined by bicinchoninic acid (BCA) method (Pierce, Rockford, IL, USA). Protein samples with the adjusted same concentration were separated by sodium dodecyl sulphate-polyacrylamide gel electrophoresis (SDS-PAGE) and loaded on polyvinylidene difluoride (PVDF) membrane (Millipore, Billerica, MA, USA). The membrane was cut into small pieces according to the molecular size and blocked in 5% skim milk for 2 h. They were incubated with primary and secondary antibodies, followed by band exposure and grey value analyses.

In Vivo Xenograft Model

This study was approved by the Animal Ethics Committee of North Sichuan Medical College Animal Center. 8-week-old male nude mice were randomly divided into two groups, and they were administrated with HCT-116 cells transfected with sh-NC (n=5) or sh-circRIP2 (n=5) in the armpit. Tumor width and length were recorded every 5 days. Mice were sacrificed at 30 days for collecting tumor tissues, which were prepared for immunostaining of CBFβ. Tumor volume (mm³) was calculated using the formula: Tumor width (mm)² × tumor length (mm)/2.

Dual-Luciferase Reporter Assay

Wild-type and mutant-type circRIP2 vectors were synthesized based on bioinformatic screening on the binding site to CBFβ. They were co-transfected in HEK293T cells with either pcDNA-NC or pcDNA-CBFβ for 48 h. Luciferase activity was finally measured in a standard method (Promega, Madison, WI, USA).

Statistical Analysis

Statistical Product and Service Solutions (SPSS) 22.0 (IBM, Armonk, NY, USA) was used for statistical analyses and data were expressed as mean ± standard deviation. Differences between groups were compared by the *t*-test. Clinical significance of NTF4 in predicting manifestations of CRC was analyzed by Chi-square test. *p*<0.05 was considered as statistically significant.

Results

Upregulation of CircRIP2 in CRC and Its Clinical Significance

Higher level of circRIP2 was detected in CRC tissues in comparison to paracancerous ones (Figure 1A). Besides, circRIP2 was upregulated in CRC cell lines as well (Figure 1B). Recruited CRC patients were divided according to T stage. QRT-PCR data revealed that circRIP2 level was higher in T3-T4 CRC cases than that of T1-T2 cases. In addition, CRC patients with distant metastasis had higher level of circRIP2

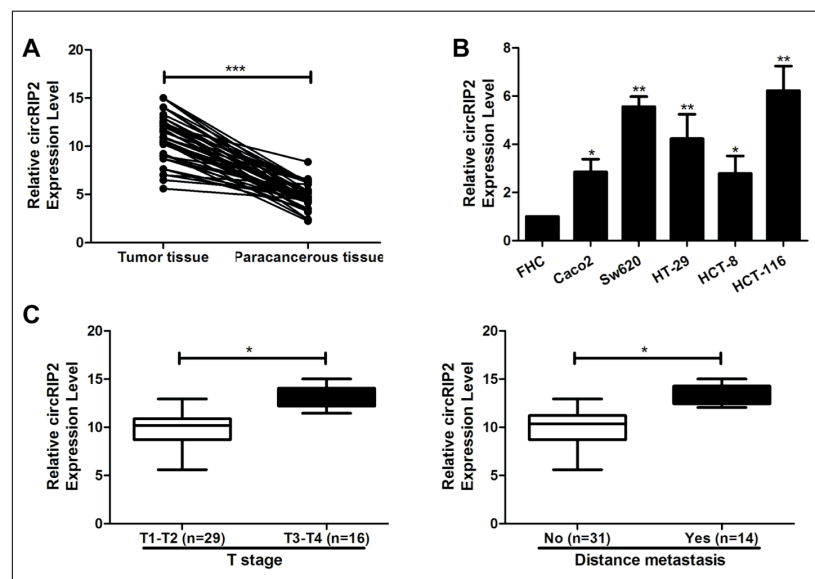


Figure 1. Upregulation of circRIP2 in CRC and its clinical significance. **A**, Differential levels of circRIP2 in CRC and paracancerous tissues; **B**, Relative level of circRIP2 in CRC cell lines; **C**, Differential levels of circRIP2 in CRC cases classified by T stage and the occurrence of distant metastasis. **p* < 0.05, ***p* < 0.01, ****p* < 0.001.

Table I. Baseline data for all the included patients with colorectal carcinoma.

Parameters	N. of cases	circRIP2 expression		p-value
		Low (n = 28)	High (n = 17)	
Age				0.912
< 60 years	19	12	7	
≥ 60 years	26	16	10	
Gender				0.672
Male	23	15	8	
Female	22	13	9	
T staging				0.011
T1-T2	29	22	7	
T3-T4	16	6	10	
Metastasis of lymph node				0.058
No	29	21	8	
Yes	16	7	9	
Distance metastasis				0.002
No	31	24	7	
Yes	14	4	10	

compared with that of non-metastatic patients (Figure 1C). Chi-square test also yielded the conclusion that circRIP2 was correlated to T stage and incidence of distant metastasis in CRC (Table I). The above data suggested that circRIP2 exerted an oncogenic role in CRC progression, which may predict tumor staging and distant metastasis of CRC.

Knockdown of Circrip2 Inhibited Proliferative and Migratory Abilities in CRC

Transfection of sh-circRIP2 markedly down-regulated circRIP2 in Sw620 and HCT-116 cells, proving its efficacy (Figure 2A). Compared with those transfected with sh-NC, cell viability was declined in CRC cells transfected with sh-cir-

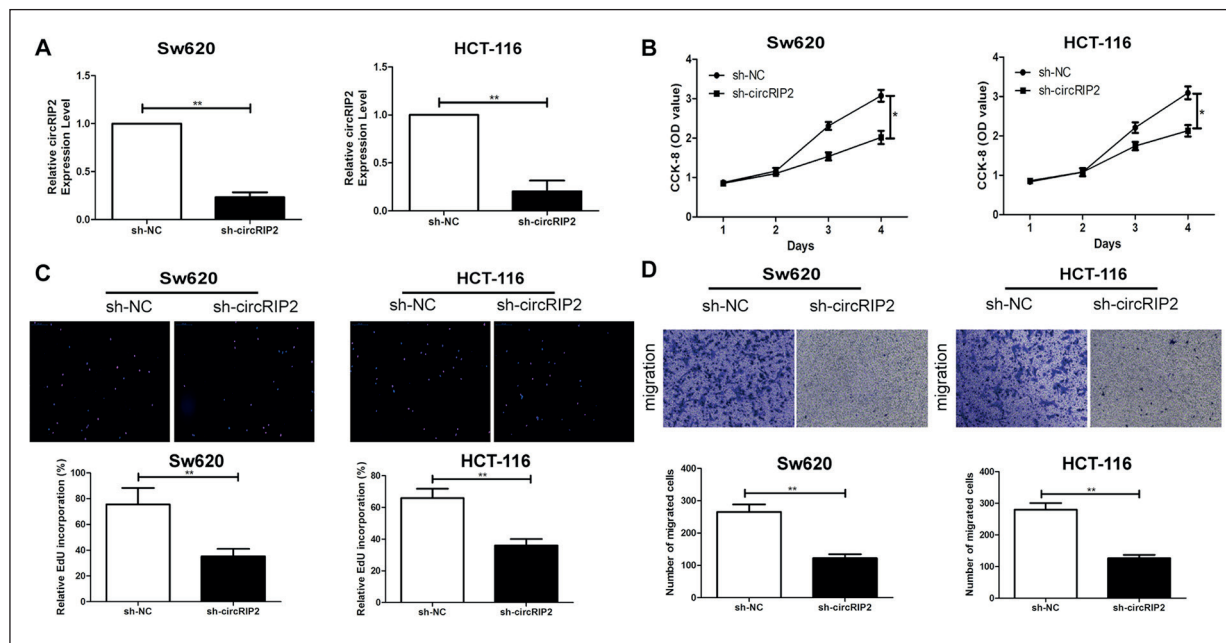


Figure 2. Knockdown of circRIP2 inhibited proliferative and migratory abilities in CRC. **A**, Transfection efficacy of sh-circRIP2 in Sw620 and HCT-116 cells; **B**, Viability in Sw620 and HCT-116 cells transfected with sh-NC or sh-circRIP2; **C**, EdU-positive rate in Sw620 and HCT-116 cells transfected with sh-NC or sh-circRIP2 (magnification 40×); **D**, Migration in Sw620 and HCT-116 cells transfected with sh-NC or sh-circRIP2 (magnification 40×). * $p < 0.05$, ** $p < 0.01$.

cRIP2 (Figure 2B). Consistently, EdU-positive rate was reduced by knockdown of circRIP2 in Sw620 and HCT-116 cells, indicating that circRIP2 promoted CRC proliferation (Figure 2C). In addition, transwell assay obtained the conclusion that knockdown of circRIP2 weakened migratory ability in CRC (Figure 2D).

CircRIP2 Was Bound to CBFB

Relative level of CBFB was upregulated by transfection of sh-circRIP2 in Sw620 and HCT-116 cells (Figure 3A). Through bioinformatic searching, a binding site was predicted in CBFB 3'UTR that could complementarily bind to circRIP2 3'UTR. Overexpression of CBFB was able to reduce Luciferase activity in the wild-type circRIP2 vector. However, CBFB did not change Luciferase activity in the mutant-type one, confirming the direct binding between circRIP2 and CBFB (Figure 3B). In CRC tissues, CBFB was lowly expressed, which was identified to negatively correlate to circRIP2 level (Figure 3C, 3D).

CircRIP2/CBFB Axis Regulated CRC Cell Phenotypes

To ascertain the interaction between circRIP2 and CBFB involved in CRC progression, we co-transfected sh-circRIP2 and si-CBFB in CRC

cells. Compared with those co-transfected with sh-circRIP2 and si-NC, CBFB was markedly downregulated in Sw620 and HCT-116 cells with co-knockdown of circRIP2 and CBFB (Figure 4A). Interestingly, co-transfection of sh-circRIP2 and si-CBFB resulted in higher viability and EdU-positive rate in CRC cells than those with solely knockdown of circRIP2 (Figure 4B, 4C). Knockdown of CBFB also enhanced migratory rate in CRC cells with circRIP2 knockdown (Figure 4D).

CircRIP2 Promoted the Tumorigenicity of CRC In Vivo

The above data have proven the *in vitro* role of circRIP2 in stimulating malignant phenotypes of CRC cells. Subsequently, its *in vivo* function in CRC growth was explored by generating a xenograft model in nude mice. Compared with mice administrated with HCT-116 cells transfected with sh-NC, those with *in vivo* knockdown of circRIP2 had a slower growth of CRC volume (Figure 5A). CRC tissues were harvested after mouse sacrifice. Downregulated circRIP2 and upregulated CBFB were detected in tumor sections collected from mice with *in vivo* knockdown of circRIP2 than those of controls (Figure 5B-5D).

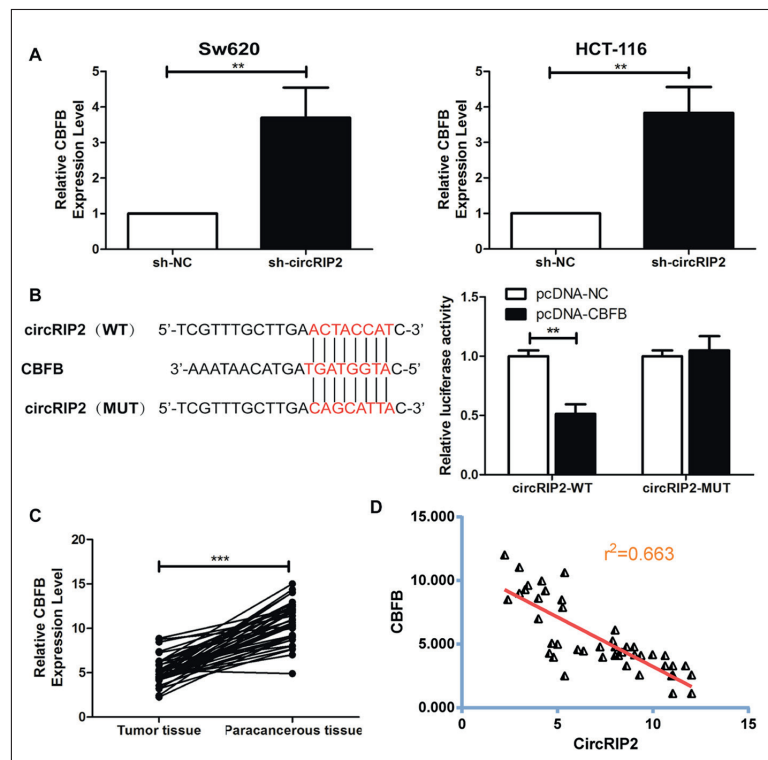


Figure 3. CircRIP2 was bound to CBFB. **A**, Relative level of CBFB in Sw620 and HCT-116 cells transfected with sh-NC or sh-circRIP2; **B**, Binding relationship between circRIP2 and CBFB; **C**, Differential levels of CBFB in CRC and paracancerous tissues; **D**, A negative correlation between circRIP2 and CBFB levels. ** $p < 0.01$, *** $p < 0.001$.

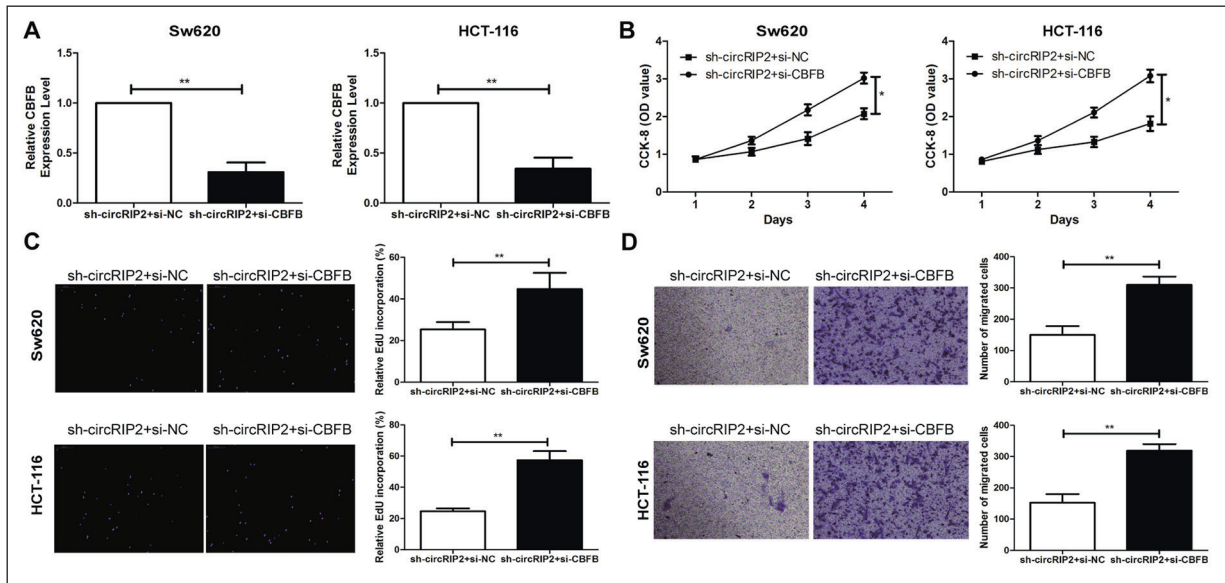


Figure 4. CircRIP2/CBFB axis regulated CRC cell phenotypes. **A**, Transfection efficacy of si-CBFB in Sw620 and HCT-116 cells transfected with sh-circRIP2; **B**, Viability in Sw620 and HCT-116 cells co-transfected with sh-circRIP2 + si-NC or sh-circRIP2 + si-CBFB; **C**, EdU-positive rate in Sw620 and HCT-116 cells co-transfected with sh-circRIP2 + si-NC or sh-circRIP2 + si-CBFB (magnification 40×); **D**, Migration in Sw620 and HCT-116 cells co-transfected with sh-circRIP2 + si-NC or sh-circRIP2 + si-CBFB (magnification 40×). * $p < 0.05$, ** $p < 0.01$.

Discussion

The incidence and mortality of CRC are on the rise not only in China, but also in the whole world¹⁻³. Surgery is still the main therapy for CRC, with the adjuvant chemotherapy and radiotherapy. The 5-year survival of CRC, howev-

er, has not been ideally enhanced⁴⁻⁶. In clinical practice, carbohydrate antigens are highly specific biomarkers for CRC screening, although their sensitivities are not ideal⁷. It is necessary to find more effective methods for screening and evaluating CRC, thereafter improving the prognosis⁸⁻¹⁰.

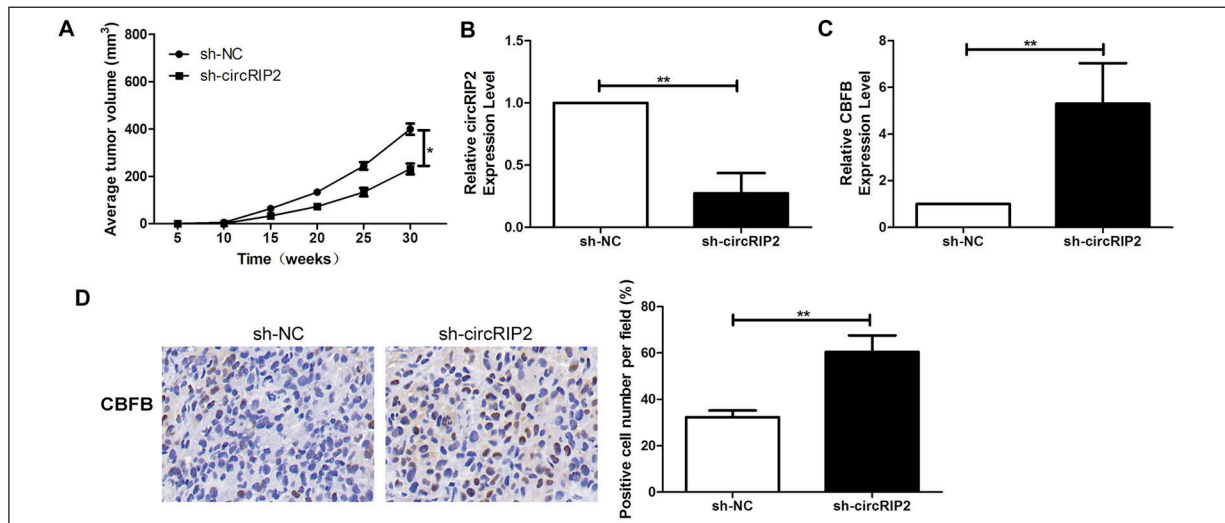


Figure 5. CircRIP2 promoted the tumorigenicity of CRC *in vivo*. Nude mice were administrated with HCT-116 cells transfected with sh-NC or sh-circRIP2. **A**, Average tumor volume from day 0 to day 30; **B**, Relative level of circRIP2 in collected tumor sections; **C**, Relative level of CBFB in collected tumor sections; **D**, Positive expression of CBFB in collected tumor sections (magnification 40×). * $p < 0.05$, ** $p < 0.01$.

CircRNAs are endogenous RNAs that can regulate gene expressions¹¹⁻¹³. They are abundantly expressed and able to affect tumor process *via* multiple mechanisms. CircRNAs are believed as promising targets that can reflect the progression of CRC¹⁴⁻¹⁶. Previously, circRIP2 is found to be linked to clinical manifestations and prognosis of bladder cancer as an oncogene¹⁷. However, the association about circRIP2 and CRC is unclear. Our results uncovered that circRIP2 was highly expressed in CRC tissues than paracancerous ones. Its level was obviously correlated to tumor staging and distant metastasis of CRC. In addition, *in vitro* knockdown of circRIP2 in Sw620 and HCT-116 cells markedly attenuated their proliferative and migratory abilities. *In vivo* knockdown of circRIP2, consistently, slowed down the growth rate of CRC in nude mice.

To further clarify how circRIP2 aggravated the progression of CRC, its potential target was predicted using bioinformatic method. CFBF was verified to bind circRIP2 as Dual-Luciferase reporter assay data demonstrated. In comparison to paracancerous tissues, CFBF was lowly expressed in CRC tissues, which was negatively correlated to circRIP2 level. Furthermore, knockdown of CFBF could reverse the inhibitory effect of lowly expressed circRIP2 on malignant progression of CRC cells. The above findings suggested that there may be a feedback loop regulation loop, that is, circRIP2 aggravated the malignant progression of CRC by negatively regulating CFBF. Therefore, our study confirmed the important effect of the circRIP2/CFBF signal axis on the progression of CRC, and the regulatory network might be a new target for the diagnosis and treatment of CRC.

Conclusions

CircRIP2 is a potential indicator for predicting tumor staging and distant metastasis of CRC. It aggravates the deterioration of CRC through negatively regulating CFBF.

Conflict of Interest

The Authors declare that they have no conflict of interests.

References

- 1) Cunningham D, Atkin W, Lenz HJ, Lynch HT, Minsky B, Nordlinger B, Starling N. Colorectal cancer. *Lancet* 2010; 375: 1030-1047.
- 2) Mattiuzzi C, Sanchis-Gomar F, Lippi G. Concise update on colorectal cancer epidemiology. *Ann Transl Med* 2019; 7: 609.
- 3) Hofseth LJ, Hebert JR, Chanda A, Chen H, Love BL, Pena MM, Murphy EA, Sajish M, Sheth A, Buckhaults PJ, Berger FG. Early-onset colorectal cancer: initial clues and current views. *Nat Rev Gastroenterol Hepatol* 2020; 17: 352-364.
- 4) McGettigan M, Cardwell CR, Cantwell MM, Tully MA. Physical activity interventions for disease-related physical and mental health during and following treatment in people with non-advanced colorectal cancer. *Cochrane Database Syst Rev* 2020; 5: D12864.
- 5) Hallajzadeh J, Maleki DP, Mobini M, Asemi Z, Mansournia MA, Sharifi M, Yousefi B. Targeting of oncogenic signaling pathways by berberine for treatment of colorectal cancer. *Med Oncol* 2020; 37: 49.
- 6) Burtin F, Mullins CS, Linnebacher M. Mouse models of colorectal cancer: Past, present and future perspectives. *World J Gastroenterol* 2020; 26: 1394-1426.
- 7) Mahar AL, Compton C, Halabi S, Hess KR, Weiser MR, Groome PA. Personalizing prognosis in colorectal cancer: A systematic review of the quality and nature of clinical prognostic tools for survival outcomes. *J Surg Oncol* 2017; 116: 969-982.
- 8) Xie YH, Chen YX, Fang JY. Comprehensive review of targeted therapy for colorectal cancer. *Signal Transduct Target Ther* 2020; 5: 22.
- 9) Yiu AJ, Yiu CY. Biomarkers in colorectal cancer. *Anticancer Res* 2016; 36: 1093-1102.
- 10) Lech G, Slotwinski R, Slodkowski M, Krasnodobski IW. Colorectal cancer tumour markers and biomarkers: Recent therapeutic advances. *World J Gastroenterol* 2016; 22: 1745-1755.
- 11) Chen LL, Yang L. Regulation of circRNA biogenesis. *RNA Biol* 2015; 12: 381-388.
- 12) Zhang HD, Jiang LH, Sun DW, Hou JC, Ji ZL. CircRNA: a novel type of biomarker for cancer. *Breast Cancer-Tokyo* 2018; 25: 1-7.
- 13) Xie R, Zhang Y, Zhang J, Li J, Zhou X. The role of circular RNAs in immune-related diseases. *Front Immunol* 2020; 11: 545.
- 14) Tang Q, Hann SS. Biological Roles and mechanisms of circular RNA in human cancers. *Onco Targets Ther* 2020; 13: 2067-2092.
- 15) Li J, Sun D, Pu W, Wang J, Peng Y. Circular RNAs in cancer: biogenesis, function, and clinical significance. *Trends Cancer* 2020; 6: 319-336.

- 16) Cui C, Yang J, Li X, Liu D, Fu L, Wang X. Functions and mechanisms of circular RNAs in cancer radiotherapy and chemotherapy resistance. *Mol Cancer* 2020; 19: 58.
- 17) Su Y, Feng W, Shi J, Chen L, Huang J, Lin T. CircRIP2 accelerates bladder cancer progression via miR-1305/Tgf-beta2/smad3 pathway. *Mol Cancer* 2020; 19: 23.
- 18) Du WW, Zhang C, Yang W, Yong T, Awan FM, Yang BB. Identifying and characterizing circRNA-protein interaction. *Theranostics* 2017; 7: 4183-4191.
- 19) Huang A, Zheng H, Wu Z, Chen M, Huang Y. Circular RNA-protein interactions: functions, mechanisms, and identification. *Theranostics* 2020; 10: 3503-3517.